Laser-Based Beam Diagnostics for a Future Linear Collider

1st Year Transfer Report

Steve Malton
University College London

June 2004

Abstract

The Laserwire is a beam profile monitor for an electron-positron accelerator. This report presents a study of the optical relay system used in analysing the laser itself, and simulations of both the optics and physics involved. The data aquisition software for the laser imaging is discussed, and results from scans taken in December 2003 are presented.

Contents

1 Introduction

The performance of a Future Linear Collider depends on control of the tranverse beam size, for example to verify beam optics and to measure transverse emittance. Expected beam sizes of 500nm $-$ $10\mu m$ mean that conventional wire scanners will be at the limit of their resolution; the wire is unable to withstand the high intensity of the electron beams.

In a Laserwire, an intense laser is focussed in the beamline. An electron bunch collides with the laser photons, which generates high energy γ-rays by Compton scattering. The electron beam is bent out of the way by dipole magnets, and the flux of γ-rays is measured.

The laser is scanned across the electron beam by a mirror mounted on a piezo-electric stack. An applied voltage of $0 - 10$V is amplified by a factor of 10, which produces an angular range of 5 mrad. By measuring the position of the laser focus and the γ-ray signal at each point, a profile of the electron beam is created.

The experiment is installed in the PETRA[1] storage ring at DESY, Hamburg.

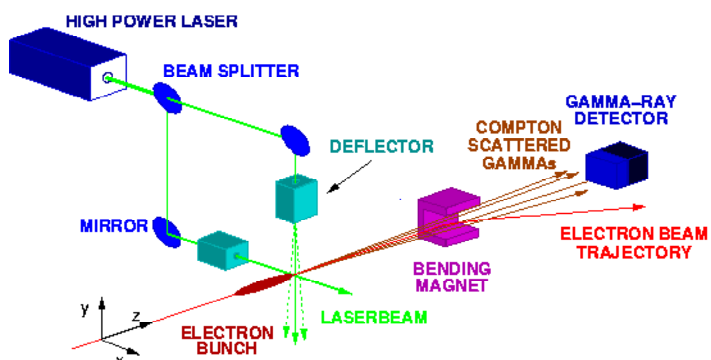

Figure 1: A simple schematic of the laserwire. At present the laser is not split, so only one axis is scanned.

1.1 Laser

The laser is a Q-switched Nd:YAG ($\lambda = 1.06\mu m$) with a Second Harmonic Generator, and a peak power of 10MW, firing at 30 Hz. The mode quality is poor, with an M^2 of 3.62, as shown in Fig. 2.

1.2 Calorimeter

The calorimeter is $PbWO_4$ crystals arranged in a 3×3 matrix, attached to a single PMT.[2] Each cell is $18 \times 18 \times 150mm$. The size is intended to detect 90% of the energy in a shower from a 350 GeV photon, as determined in simulations within Geant4[3]. $PbWO_4$ is chosen for its fast decay time, small Moliere radius

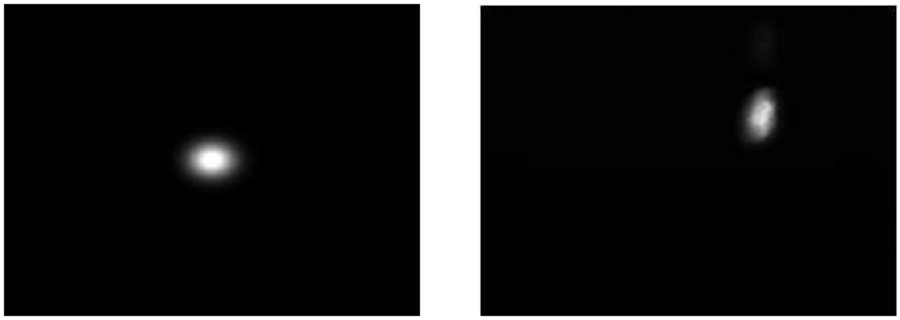

Figure 2: The actual laser pulse(right) alongside a pure TEM_{00} mode, which has $\mathrm{M}^2 = 1$. This is gaussian in x and y.

and short interaction length. This combination keeps the detector compact and reduces signal pile-up.

1.3 Beam Position Monitor

The beam position monitor near the interaction point is composed of four pickup plates. When a charged particle bunch passes the plates, a voltage is induced, the size of which is related to the distance to the bunch by:

$$x = K_x \frac{(U_1 + U_4) - (U_2 + U_3)}{U_1 + U_2 + U_3 + U_4} \tag{1}$$

$$y = K_y \frac{(U_1 + U_2) - (U_3 + U_4)}{U_1 + U_2 + U_3 + U_4} \tag{2}$$

where $\mathrm{K}_{x/y}$ are machine constants, and U_i is the voltage in the i^{th} pickup.

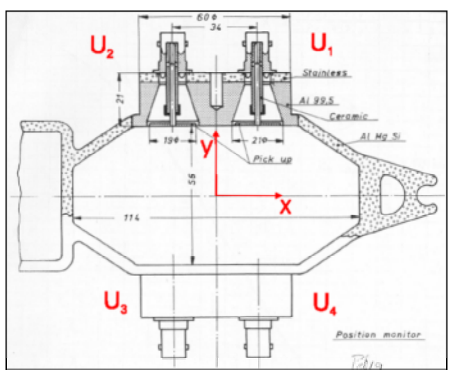

Figure 3: The beam position monitor pickup arragement near the laserwire interaction point.[4]

2 Physics Overview

The number of Compton photons produced per bunch crossing is proportional to the integral of the overlapping density functions of the electron beam and the laser. For the simplified case, where both beams are assumed to be Gaussian in cross-section, and constant in the direction of motion, it can be shown that the photon count per bunch is:

$$N_c = N_b \frac{P_L \sigma_c \lambda}{c^2 h} \frac{1}{\sqrt{2\pi\sigma_s^2}} \exp\left(\frac{-(\Delta y)^2}{2\sigma_s^2}\right) \tag{3}$$

where $\sigma_s^2 = \omega_0^2 + \sigma_y^2$.[5, 6], the quadratic sum of the laser and electron beam sizes.

2.1 Compton Scattering

At first order in α, the process $e^- + \gamma \rightarrow e^- + \gamma$ has two diagrams, (Fig. 4).

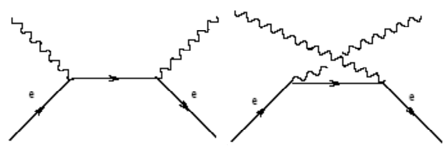

Figure 4: First order diagrams for $e^- + \gamma \rightarrow e^- + \gamma$.

Up to a maximum energy $\omega_{max} = \frac{2\epsilon}{1+2\epsilon}$, the cross-section for Compton scattering is:

$$\frac{d\sigma}{d\omega} = \frac{3\sigma_0}{8}\left[1 - \omega + \frac{1}{1-\omega} + \left[\frac{\omega}{\epsilon(1-\omega)}\right]^2 - \frac{2\omega}{\epsilon(1-\omega)}\right] \tag{4}$$

where $\omega = \frac{\nu}{E_b}$ is the normalised photon energy, and $\epsilon = \gamma\frac{\nu_0}{m_e}$ is the energy of a photon in the electron rest frame in units of the electron rest mass, in natural units.

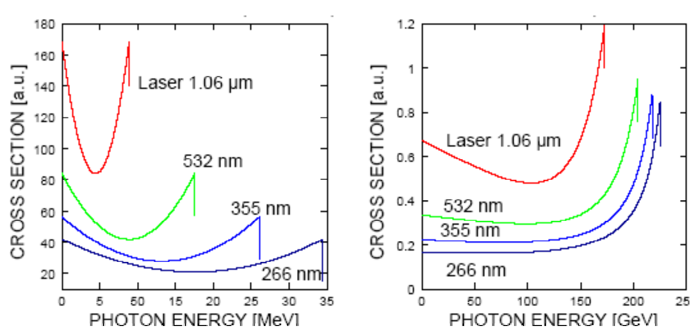

Figure 5: Energy spectra of Compton scattered photons at four wavelengths. The incident electron energies are 1 GeV (left) and 250 GeV (right).

2.2 Gaussian Beams

We assume the intensity profile of the laser to be gaussian about the beam axis:

$$I(r) = I_0 \exp\left(\frac{-2r^2}{\omega^2}\right) = \frac{2P_L}{\pi\omega^2} \exp\left(\frac{-2r^2}{\omega^2}\right) \tag{5}$$

where ω is the beam spot size; this is the radius at which the intensity falls to $1/\mathrm{e}^2$ of its peak value.

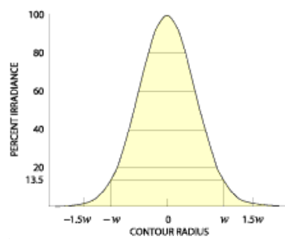

Figure 6: The intensity distribution of the laser as a function of radius. [7]

Diffraction causes light waves to spread transversely as they propogate, so the perfectly collimated beam that has been assumed in deriving Eqn. 3 diverges, and the spot size of the laser beam at a distance z from the waist is:

$$\omega^2 = \omega_0^2 \left[1 + \left(\frac{M^2 \lambda z}{\pi \omega_0^2}\right)^2\right] \tag{6}$$

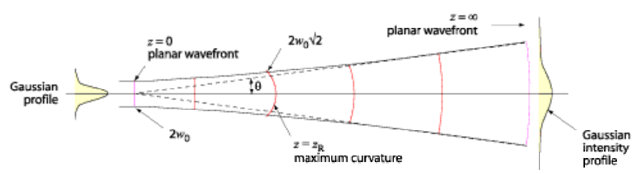

Figure 7: The variation of beam radius along the direction of propogation. [7]

3 Optical System

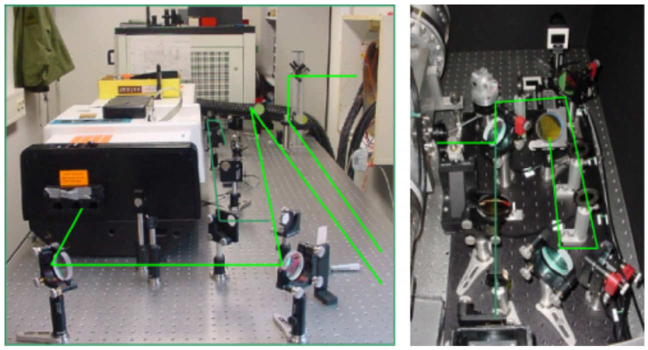

Figure 8: The optical path prior to the interaction point.

3.1 CCD

The laser is profiled on Basler A302fs CCD cameras.[8] The chip is 782×582 pixels, with a pitch of $8.3\mu m$. One is located prior to the interaction point, and another after; both are behind splitters to reduce the laser intensity to levels which will not damage the camera. The cameras are read out to an IEEE1394 Firewire bus on a PC running Windows 2000(SP4).

Figure 9: Basler A300 (left) and A600 series digital cameras. The objective lenses are removed and another optical system is used for focussing.

Due to the high level of synchrotron radiation at the camera location in PETRA, it is possible that the A302fs may be replaced with A601f. These are CMOS cameras, rather than CCD, and are much more radiation hard.

3.2 CCD DAQ

The imaging software is written in Visual C++ 6.0, using the Microsoft Foundation Classes. Images are captured at 25–30 frames per second, and written to disk as .bmp files. The program automatically detects the number of cameras, and displays images from each in separate windows. Statistics for the selected window, such as frame rate and saturated pixel count are updated in the status bar of the main window.

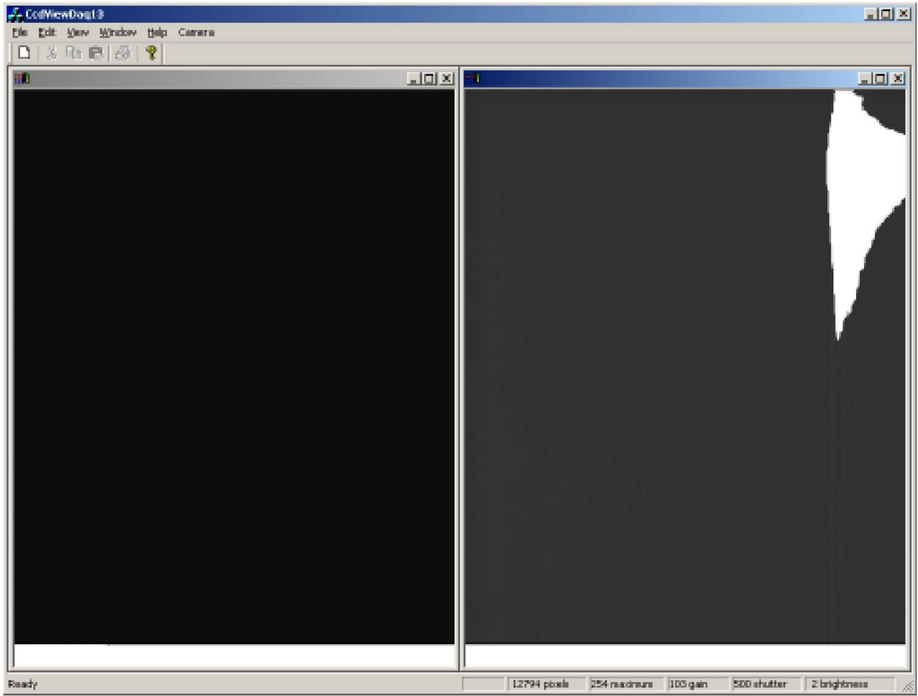

Figure 10: Screenshot of the CCD DAQ software running on two cameras. The statistics displayed in the status bar refer to the window with focus — in this case, on the right.

The program continually listens for a socket connection. In this way, it can receive commands (Table 1) to start and stop taking data from a control program. The command to start precedes a timestamp, which is incorporated into the names of the files as they are written to disk.
The control program, built in LabView[9], sends commands to the BPM, calorimeter and CCD DAQ programs to take data at each scan point between movement of the piezo-scanner.

LW_INIT_HARD
LW_TAKE_DATA
LW_STOP_DATA
LW_TERM_HARD
LW_TERM_PROC

Table 1: The commands which can be sent by the control program. The CCD DAQ only recognises the _DATA messages, ignoring others.

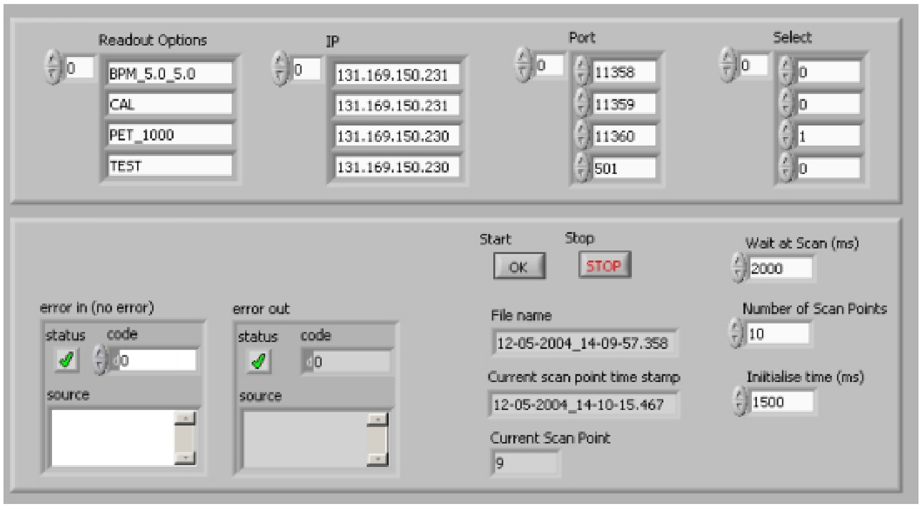

Figure 11: A screenshot of the control program.

4 Simulations

4.1 Optics

From Equation 3, it is clear that we need a good understanding of the profile of the laser, and how well the waist at the interaction point is imaged at the CCD. Here I explore the translation of the waist as the scanner cahnges position, and the magnification of the optical system after the interaction point.

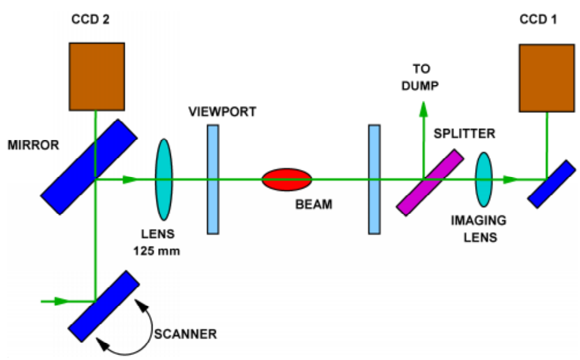

Figure 12: A diagram of the optical path from the piezo-scanner to the CCD through the interaction point.

4.1.1 At the Interaction Point (IP)

The complex radius of curvature, q, of a Gaussian beam transforms as $\frac{1}{q_1} = \frac{C+D\frac{1}{q_0}}{A+B\frac{1}{q_0}}$ where A,B,C and D are the elements of the system matrix

$$M_{sys} = M_n\, M_{n-1} \ldots M_2\, M_1 = \prod_{r=n}^{1} M_r \tag{7}$$

and M_n is the paraxial ray transformation matrix of the n^{th} optical element. For $\Re\{1/q\} = 0$, the beam is waisted and $\Im\{1/q\} = -\pi\omega^2/\lambda$ gives the beam spot size, ω, at the waist location.

Taking the scanning mirror as the initial beam waist location, the beam propogates 125mm to the pre-IP splitter, then a further 85mm to an LAP125 air-spaced doublet lens[10], before a final 119mm propogation to the the IP, (Fig. 12. Calculating the system matrix from Eq. 7, the position, y', and angle, α', of the laser at the IP can be calculated from:

$$\begin{pmatrix} y' \\ \alpha' \end{pmatrix} = \begin{pmatrix} A & B \\ C & D \end{pmatrix} \begin{pmatrix} y \\ \alpha \end{pmatrix} \tag{8}$$

For $y = 0$, and an initial range $-2.5mrad \leq \alpha \leq 2.5mrad$, we determine y' values, that is, focus translation at the IP, as shown in Fig. 13. For a 1mm input spot size, the waist at IP becomes $20.94\mu m$.

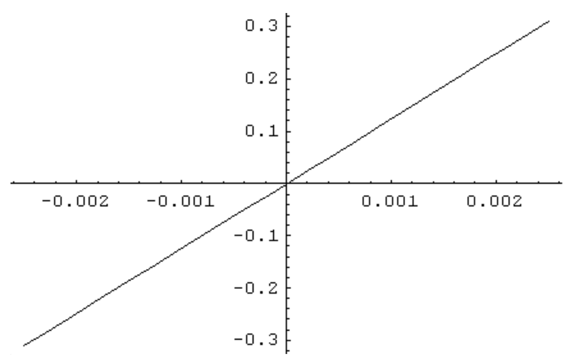

Figure 13: Focus position at the IP (mm) vs. angle of scanning mirror (radians). This shows a linear response of $62.0\mu m$ per volt, for $0 \leq \mathrm{V} \leq 10\mathrm{V}$.

4.1.2 Post-IP

Having determined the system matrix for propogation from the scanning mirror to the IP, it is simple to include propogation to the post-IP CCD through a 4f relay of a PAC076 triplet lens[10]. Taking the thickness of the lens into consideration, this makes for IP–lens and lens–CCD spacing of 185.9mm. Again for $y = 0$, $-2.5mrad \leq \alpha \leq 2.5mrad$, beam spot translation at the CCD is shown in Fig 14. The imaged spot size for a 1mm input beam is $20.93\mu m$.
From simple lens formulae, the magnification $m = \frac{|v|}{u}$, where v and u are the image and object distances, respectively. For a 4f relay, where $v = u = 2f$, as above, this gives a 1:1 image size ratio. However, this requires perfect placement of the PAC076 lens exactly 2f from the waist at the IP. Therefore it is not certain that the imaging ratio is 1:1. It is proposed to solve this by using a 2 lens system.

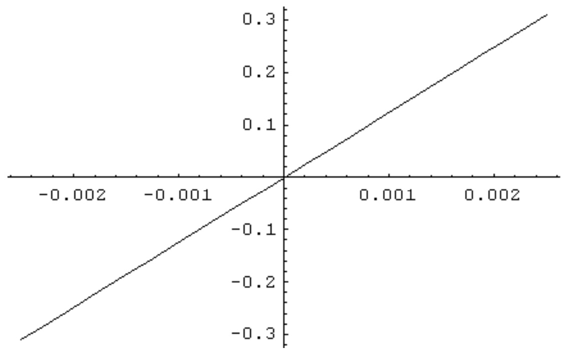

Figure 14: Focus position at CCD (mm) vs. angle of scanning mirror (radians). The result is almost perfect imaging of the beam spot at the IP.

A collimating lens is placed 1f from the IP, and the beam is brought to a focus 1f from a second lens. In this case, the laser will be collimated only when the first lens is correctly placed. By sampling the beam spot size at several locations, the collimation can be tested.[1]

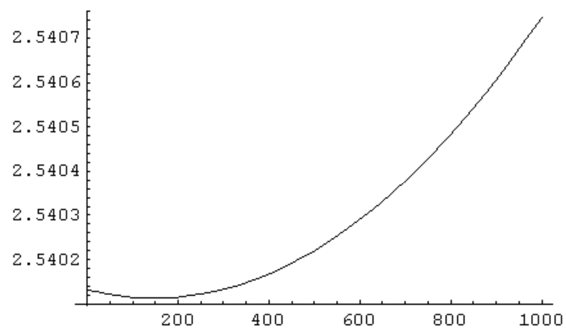

Figure 15: The variation in beam waist (mm) after a 150mm focal length lens, from an initial beam spot size of $10\mu m$. Note that the beam is collimated to within $1\mu m$ over 1m.

Once the beam is collimated over a large range, the second lens, of the same focal length as the first, can be placed anywhere in the beam; testing for collimation may require a large distance, but once verified, the location of the second lens is a matter of convenience.

With both lenses in place, it is only the placement of the CCD that remains. The correct location may be acheived by minimising the spot size on the CCD — the correct location is at the waist, so being misplacement will increase the image size.

[1]At this point, the beam radius is significantly larger than the wavelength,so beam divergence is negligible.

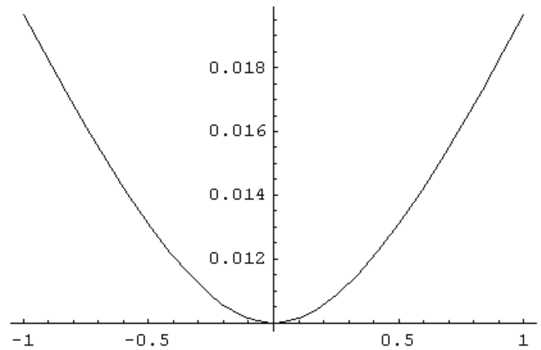

Figure 16: The variation in image spot size (mm) with offset from the ideal CCD location (mm).

For direct imaging of the laser pulse, the image size is only a few pixels. To observe the cross-section of the laser in greater detail, the focal length of the second lens can be increased. This increases the image size as:

$$\omega \propto M^2 \lambda f \tag{9}$$

4.2 Compton Scattering

Equation 3 gives the number of Compton photons as a function of the offset between the laser and the electron bunch, where both beams are taken to be cylinders of constant radius. Here, the waist in Equation 6 is used as the radius of the laser, allowing it to vary along the beam axis. The electron beam is also given a moving bunch structure, so the overlap integral becomes:

$$N_\gamma \propto \int dV \int_{-\infty}^{\infty} dt \exp\left[-\frac{(z-ct)^2}{2\sigma_z^2} - \frac{x^2}{2\sigma_x^2} - \frac{y^2}{2\sigma_y^2} - \frac{(y-y_0)^2 + z^2}{2\omega_0^2\left[1 + \left(\frac{M^2\lambda(x-x_0)}{\pi\omega_0^2}\right)^2\right]}\right] \tag{10}$$

where V extends over all space in y and z, and over the length of the laser pulse, $\pm c\tau_L/2$, in x.

At this point, the integral of the overlap function becomes impossible to solve analytically. To make a numerical approximation, the product is sampled over a range of 2σ in steps of $\frac{\sigma}{5}$ in space, and $2\tau_e$ in steps of $\frac{\tau_e}{/5}$ in time.This is repeated for a range of beam offsets, and for the case in which the waist of the laser is not focussed correctly onto the electron bunch. The results are shown in Fig. 17, using the values in Table 2.

λ	M^2	$\sigma_{e\,x/y}$	$\sigma_{e\,z}$	σ_γ	E_b	N_e	P_L
532 nm	3.62	20 μm	12.75 mm	10 μm	6 GeV	8 10^{10}	10 MW

Table 2: Parameters used in simulating the Compton signal.

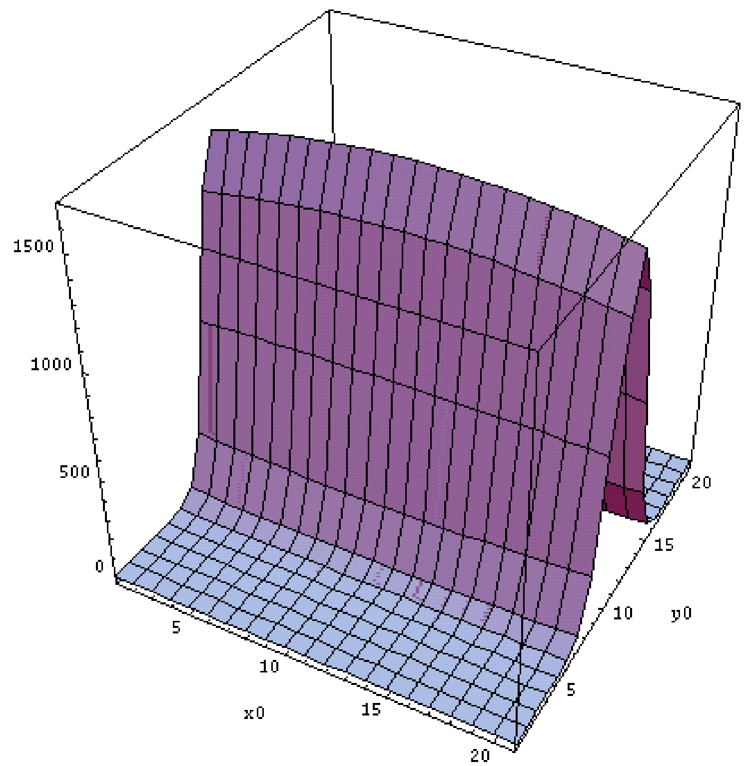

Figure 17: The total energy deposited in the calorimeter (GeV) against beam offset y_0 and waist position x_0. Each division is 2 μm, with zero offset being at position 11.

5 CCD Calibration

Direct measurement of the laser waist is not possible at PETRA, where the focal point is inside the beamline. A smaller model system is in place at Royal Holloway, and this is used to calibrate the CCDs.

A razor blade is stepped through a He:Ne laser beam by computer-controlled picomotors. The blade position is measured by an interferometer which counts fringe motion by measuring periodic intensity variation on a photodiode.

For a TEM_{00} beam, the intensity at a photodiode after the razor will vary as:

$$I \propto \frac{1}{2}(1 + Erf[x]) \tag{11}$$

The differential with respect to x gives the intensity distribution in the x direction.

The razor is also on a platform for travel in the beam direction. The measured beam radii can then be fitted to Eq. 6. The minimum waist can then be compared to the analysis of the images from the CCD. This work is underway at present.

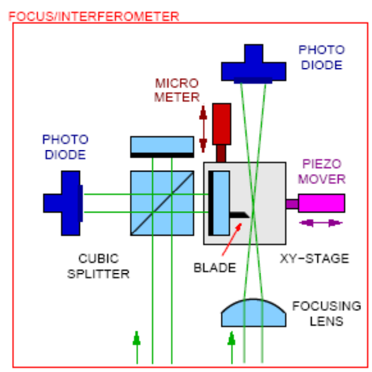

Figure 18: Diagram of the knife-edge scan interferometer at RHUL.

6 Scan Results

6.1 Laser profile

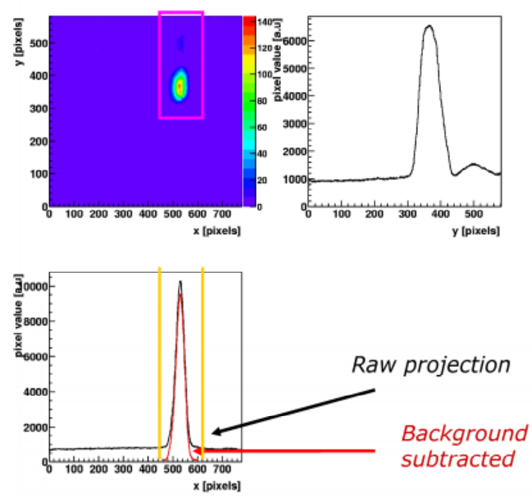

Figure 19:

Analysis of the CCD images is done in ROOT[11]. The bitmap is loaded into a 2D histogram, and the x and y projections are taken. After background subtraction, these projections are fitted to a gaussian to calculate mean position and rms.

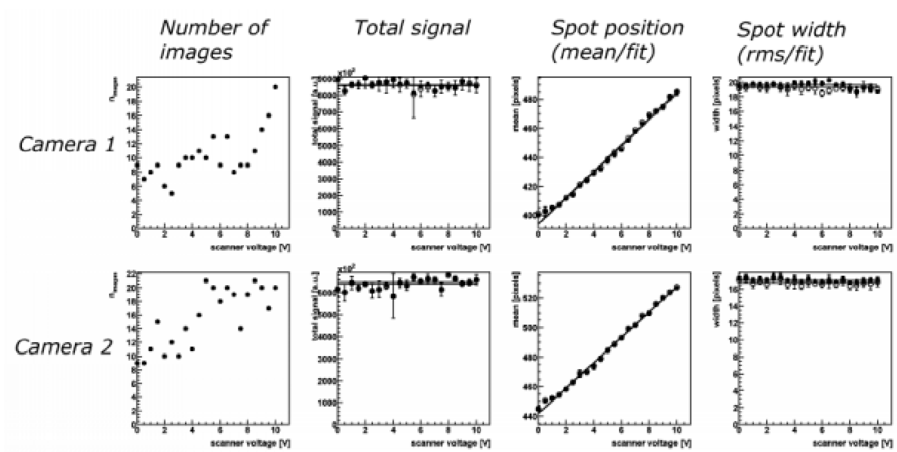

Figure 20: Analysis of the CCD data for the low current run, 7.1mA. From left to right: Number of images, total intensity, spot position, and laser rms vs applied scanner voltage.[12]

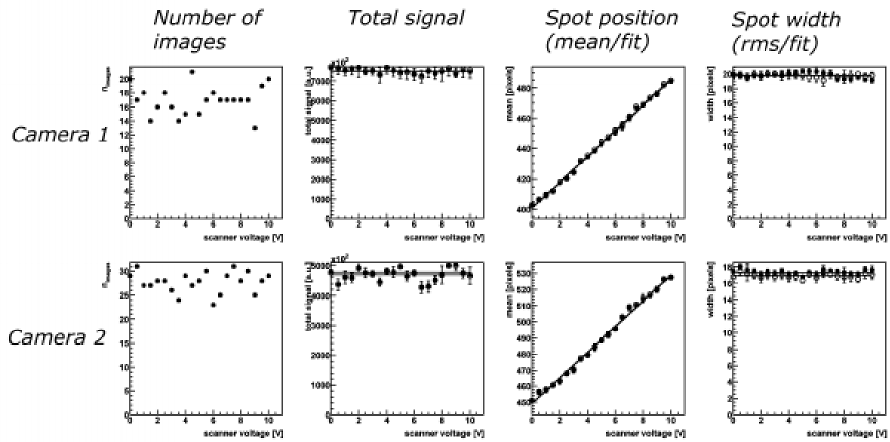

Figure 21: Analysis of the CCD data for the high current run, 40.5mA. From left to right: Number of images, total intensity, spot position, and laser rms vs applied scanner voltage.[12]

6.2 Electron Beam Profile

To take the scan, the piezo-scanner is set to the 5V position, and the electron beam is moved into the laser by means of steering magnets. Once the position is set, the scanner is stepped from 0–9.5V in steps of 0.5V. Data from the calorimeter, CCDs and beam position moniter are stored for offline reconstruction of the beam profile.

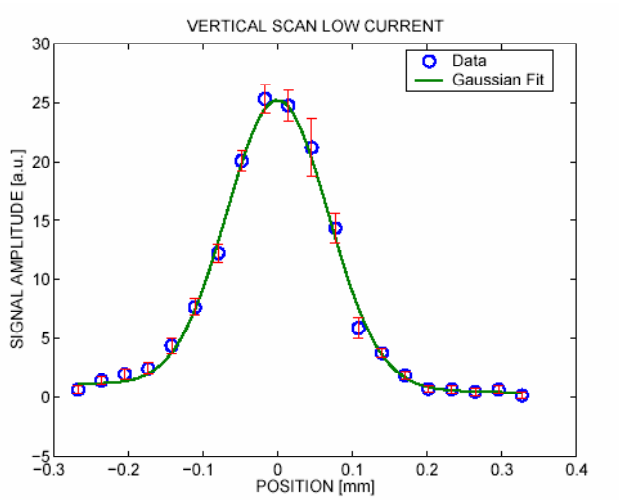

Figure 22: Results from Dec.03. Beam current 7.1mA, first bunch 3.9nC. [13]

Using data from the Laserwire run in December, we measure a beam size of $\sigma = (68 \pm 3 \pm 14)\,\mu m$ at low current (Fig. 22), and $\sigma = (80 \pm 6 \pm 16)\,\mu m$ at

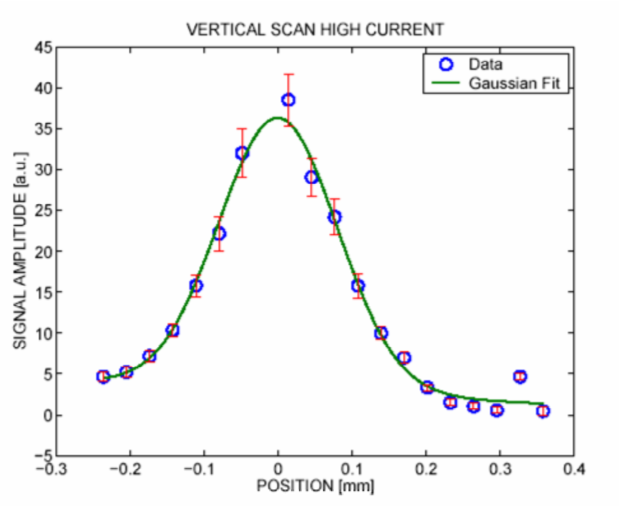

Figure 23: Results from Dec.03. Beam current 40.5mA, first bunch 22.3nC. [13]

high current (Fig. 23). The results are slightly sloping; this is because of the length of time taken to perform the scan, during which the beam current in PETRA decreased.

7 Future Work

• CCD DAQ upgrades:
Add command buttons for start/stop grabbing.
Add sliders for gain/brightness/shutter variation.
Add scroll bars to view windows in the case that the image is larger than the window OR
Scale images to fit in reduced window size.
The CCDs are running untriggered at present. With the laser firing at 30 Hz, and the CCDs capturing at 25–30 fps, this means that many images are blank, taken when the laser is off. The CCDs need to be triggered to ensure that as many images as possible contain data.

• Fast Scanning:
The piezo-scanner is capable of operating at 10 kHz. A fully automated system should be able to take scans in a much shorter time.

• Position Simulations:
An understanding of the most efficient locations for a laserwire in the Beam Delivery System of a future linear collider is required, along with detailed studies of the effect that the laserwires may have on the beam downstream of the scanning point.

References

[1] PETRA, http://www-hasylab.desy.de/facility/main.htm

[2] G. Blair et al, "R&D Towards a Laser Based Beam Size Monitor for the Future Linear Collider", Presented at EPAC 2002

[3] K. Amako, [Geant4 Collaboration], "Present Status of Geant4", Nucl. Instrum. Meth. A 453 (2000) 455

[4] J. Keil, HERA Beam Dynamics Seminar, July 2003

[5] P. Tenembaum and T. Shintake, "Measurement of Small Electron-Beam Spots", Annu. Rev. Nucl. Part. Sci. 1999.49:125-62

[6] K. Balewski et al, "Simulation and Background Measurements for a Laser Based Beam Size Monitor for the Future Linear Collider", Proceedings of the 2001 Particle Accelerator Conference, Chicago

[7] Melles-Griot Gaussian beam tutorial, http://beammeasurement.mellesgriot.com/tutorial.asp

[8] Basler A300 series specifications, http://www.multipix.com/PDF/A300.pdf

[9] National Instruments, http://www.ni.com

[10] ZEMAX lens library, ZEMAX Development Corporation, http://www.zemax.com

[11] CERN ROOT Collaboration, http://root.cern.ch

[12] S. Boogert, Laserwire UK meeting, Oxford, 16^{th} Jan. 2004

[13] T. Kamps, Laserwire UK meeting, Oxford, 16^{th} Jan. 2004

Some general references:

• LBBD Collaboration,
http://www.hep.ph.rhul.ac.uk/~kamps/lbbd/

• A. E. Siegman, Stanford University,
University Science Books, 1986